Physics Letters A 373 (2008) 169–172

Contents lists available at ScienceDirect

Physics Letters A

www.elsevier.com/locate/pla

Complete evanescent tunneling gaps in one-dimensional photonic crystals

T.B. Wang, J.W. Dong, C.P. Yin, H.Z. Wang *

State Key Laboratory of Optoelectronic Materials and Technologies, Zhongshan (Sun Yat-Sen) University, Guangzhou 510275, China

ARTICLE INFO

Article history:
Received 11 June 2008
Received in revised form 24 October 2008
Accepted 28 October 2008
Available online 5 November 2008
Communicated by R. Wu

PACS:
41.20.Jb
42.70.Qs
78.20.Ci

Keywords:
Photonic crystals
Single-negative materials

ABSTRACT

Complete band gaps are found in one-dimensional photonic crystals composed of negative-permittivity and negative-permeability materials. The mechanism of these complete band gaps, unlike the Bragg complete gaps formed by interferences of forward/backward propagating waves, originate from the evanescent wave tunneling in the single-negative materials is reported for the first time. Moreover, it is also reported for the first time that both Bragg complete gaps and evanescent wave tunneling complete gaps exist in a three-constituent one-dimensional photonic structure simultaneously.

1. Introduction

Photonic crystals (PCs) are artificial materials with periodically modulated dielectric function, which can create a range of forbidden frequencies called photonic band gaps because of Bragg scatterings [1–3]. PCs have many potential applications because of their novel properties, e.g., manufacturing omni-directional reflectors, controlling spontaneous emission in quantum devices and manipulating light in photonic information technologies.

It is known, in the past, that three-dimensional complete gaps just exist in three-dimensional photonic crystals (PCs), which are difficult to fabricate. Since omni-directional band gap of one-dimensional (1D) PCs was proposed in 1998 [4], extensive attentions have been attracted and many applications about this omni-directional band gap have been developed [4–7]. However, until now it is still impossible to achieve complete gaps (i.e. complete gaps in the whole momentum space inside the crystal) in 1DPCs that are composed of positive refraction index materials (PIMs).

Recently, the extraordinary properties of negative refraction index materials (NIMs) [8] attract plenty of researches and many interesting works about these novel materials have been reported [9–18]. Among them, it is reported firstly that complete gaps can appear in the 1DPC contains NIMs by Shadrivov et al. [13]. The authors in Ref. [13] design a 1DPC consisting of three alternating layers made of PIMs and NIMs which possesses a complete three-dimensional band gap, which originates from Bragg scattering.

In this Letter, we proposed another kind of complete gap in the 1DPC consisting of single-negative (SNG) materials. We found that the existence of such complete gaps is caused by the evanescent wave tunneling in SNG materials. We also designed a three-constituent 1DPC that possesses both Bragg-scattering-assisted and evanescent-wave-assisted complete gaps simultaneously for both transverse electric (TE) and transverse magnetic (TM) polarizations. At the end of the Letter, we discussed the possible application of appearing complete gap in the visible.

2. Model and theory analysis

Consider the 1DPC with the periodic structure of $(AB)^N$ where A and B represent two types of SNG materials and N is the number of periods. The periodic structure coupled to a homogeneous medium, characterized by n_0, at the interface. Electromagnetic waves are incident upon the 1DPC from the homogeneous medium. We assume the z axis is along the normal to the interfaces and the wave vector component parallel to the layers $k_{\parallel}$ is along the y axis. For TE wave, the electric field $\vec{E}$ is in the reverse direction of y axis, and for TM wave, the magnetic field $\vec{H}$ is in the y direction, as shown in Fig. 1. The electric and magnetic fields at any two positions z and $z+\Delta z$ in the same layer can be related by transfer matrix [12,13,19]

$$M_i(\Delta z) = \begin{pmatrix} \cos(k_i \Delta z) & -\frac{1}{\sigma_i}\sin(k_i \Delta z) \\ \sigma_i \sin(k_i \Delta z) & \cos(k_i \Delta z) \end{pmatrix} \quad (i = \mathrm{A}, \mathrm{B}), \tag{1}$$

* Corresponding author.
E-mail address: stswhz@mail.sysu.edu.cn (H.Z. Wang).

0375-9601/$ – see front matter
doi:10.1016/j.physleta.2008.10.076

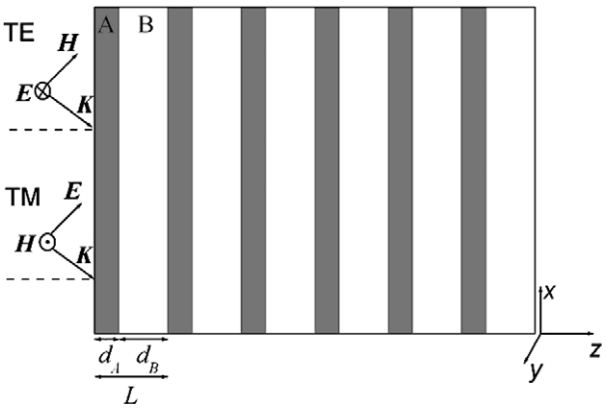

Fig. 1. Schematic representation of the finite dispersive multilayered periodic structure.

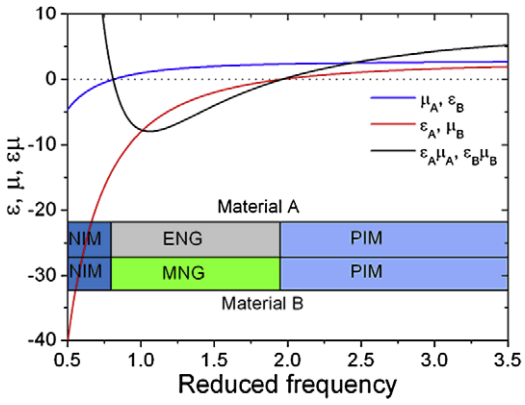

Fig. 2. Relationship between frequency and the parameters of materials A and B.

where $k_i = (\omega^2\varepsilon_i\mu_i/c^2 - k_\parallel^2)^{1/2}$, $\sigma_i = k_i/\mu_i$ for TE wave and $\sigma_i = k_i/\varepsilon_i$ for TM wave.

For an infinite periodic structure, according to the Bloch's theorem, the dispersive relation can be written as [12,13]

$$\cos(KL) = \cos(k_A d_A)\cos(k_B d_B) - \frac{1}{2}\left(\frac{\sigma_B}{\sigma_A} + \frac{\sigma_A}{\sigma_B}\right)\sin(k_A d_A)\sin(k_B d_B), \quad (2)$$

where K is the Bloch wave vector, d_A and d_B is the thickness of layer A and layer B respectively, $L = d_A + d_B$ is the width of one period. The condition of Eq. (2) having no real solution for $k_\parallel$ is $|\cos(KL)| > 1$, which corresponds to the band gaps of the 1DPC. If $|\cos(KL)|$ is always larger than 1 for all $k_\parallel$, that denotes the Bloch wave vector K remains complex for all real $k_\parallel$, then a complete gap occurs [13].

3. Numerical calculation and discussion

The relative permittivity and permeability of the SNG materials in this Letter are given by the Drude model [20]

$$\varepsilon_i = \varepsilon_{0i} - \frac{\omega_{ep,i}^2}{\omega^2},$$
$$\mu_i = \mu_{0i} - \frac{\omega_{mp,i}^2}{\omega^2}, \quad i = A, B, \quad (3)$$

where $\varepsilon_{0i}(\mu_{0i})$ and $\omega_{ep,i}$ ($\omega_{mp,i}$) are the effective static electric (magnetic) constants and the effective electric (magnetic) plasma frequencies, respectively. In this Letter, we choose $\varepsilon_{0i} = \mu_{0i} = 2.828$, $(\omega_{ep,A}L/c)^2 = (\omega_{mp,B}L/c)^2 = 428.8$, $(\omega_{mp,A}L/c)^2 = (\omega_{ep,B}L/c)^2 = 73.6$, c is the speed of light in vacuum. This model can be realized in artificial designed transmission lines [20–22]. For convenience, we substitute $\omega L/c$ with Ω as reduced frequency. The relationships on permittivity, permeability, and their product as a function of reduced frequency are shown in Fig. 2. In the following, we distinguish our discussion into three frequency ranges according to the signs of permittivity and permeability.

(i) $\Omega > 1.96$. In this frequency range, both materials A and B are PIMs, i.e., $\varepsilon_i > 0$, $\mu_i > 0$ ($i = A, B$). The product of permittivity and permeability ($\varepsilon\mu$) is a positive number, as shown is Fig. 2. The value of σ_A/σ_B is also a positive number. As is well known, there are no complete band gaps in this frequency range.

(ii) $\Omega < 0.812$. In this frequency range, both materials A and B are NIMs, i.e., $\varepsilon_i < 0$, $\mu_i < 0$ ($i = A, B$). The product of permittivity and permeability ($\varepsilon\mu$) is a positive number as shown in Fig. 2. The value of σ_A/σ_B also has a positive sign. According to Eq. (2), we can find that the dispersive relation mainly depends on the signs of $\varepsilon\mu$ and σ_A/σ_B. Because $\varepsilon\mu$ and σ_A/σ_B have the same signs as that in the range of $\Omega > 1.96$, the same dispersive relation is in this frequency range as that in the range above $\Omega > 1.96$. Therefore, there are also no complete band gaps in this frequency range.

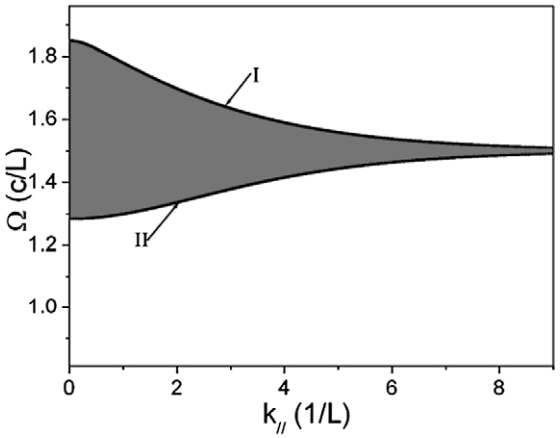

Fig. 3. Magnitudes of $|\cos(KL)|$ as a function of reduced frequency and parallel wave vector, the grey area corresponds to $|\cos(KL)| < 1$ and the white area is $|\cos(KL)| > 1$, the black line denotes $|\cos(KL)| = 1$.

(iii) $0.812 < \Omega < 1.96$. Materials A, B are epsilon-negative (ENG) ($\varepsilon_A < 0$, $\mu_A > 0$) and mu-negative (MNG) ($\mu_B < 0$, $\varepsilon_B > 0$), respectively. Thus, $k_A = k_B$ becomes an imaginary number. In this case, the dispersive relation (TE polarization) of Eq. (2) can be written as

$$\cos(KL) = \cosh(|k_A|d_A)\cosh(|k_B|d_B) - \frac{1}{2}\left(\frac{|\mu_B|}{|\mu_A|} + \frac{|\mu_A|}{|\mu_B|}\right)\sinh(|k_A|d_A)\sinh(|k_B|d_B).$$

Fig. 3 shows magnitudes range of $|\cos(KL)|$ as a function of reduced frequency Ω and parallel wave vector $k_\parallel$, the grey and white area represent $|\cos(KL)| < 1$ and $|\cos(KL)| > 1$, respectively, the black line is $|\cos(KL)| = 1$. One can see that, the black line I moves to lower frequency when $k_\parallel$ getting larger, and the black line II moves to upper frequency when $k_\parallel$ getting larger. They tend to a constant frequency. Therefore, the value of $|\cos(KL)|$ in white area is always lager than 1 for all $k_\parallel$, i.e., there exist complete gaps in this frequency range.

4. Complete gaps IN 1DPC composed of ENG–MNG

Because $\varepsilon_A = \mu_B$, $\mu_A = \varepsilon_B$, one can get the same dispersive relation for TE and TM waves by using Eq. (2). The band structure is symmetrical for both polarizations. In Fig. 4, we plot the

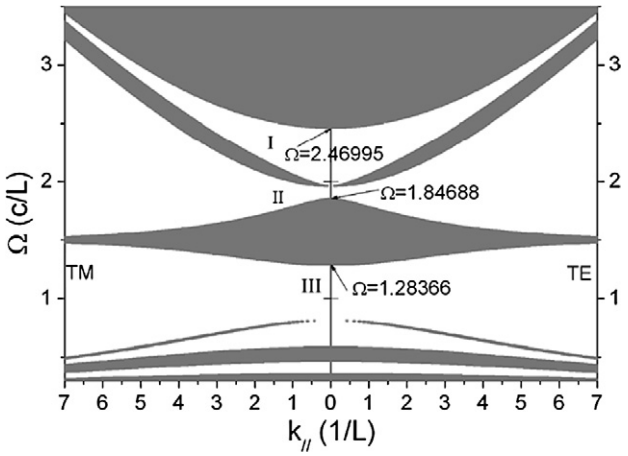

Fig. 4. Projected band structure of one-dimensional photonic crystal composed of single-negative materials with the parameters: $d_A = d_B = 0.5L$.

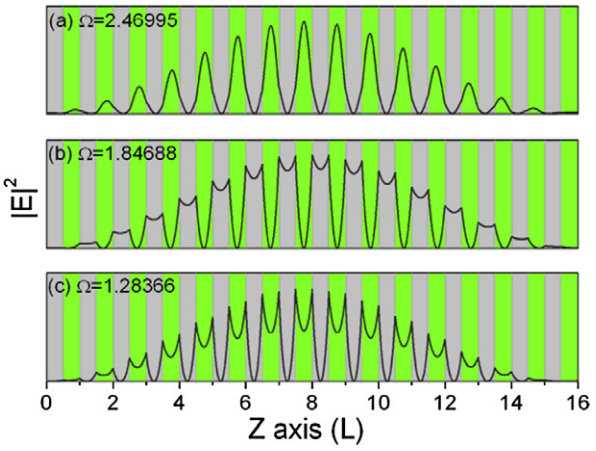

Fig. 5. Electric fields inside the 1DPC of $(AB)^{16}$ at different frequencies: (a) $\Omega = 2.46995$ is the up band edge of gap I in Fig. 4. (b) $\Omega = 1.84688$ is the low band edge of the gap II in Fig. 4. (c) $\Omega = 1.28366$ is the up band edge of the gap III in Fig. 4.

projected band structure of 1DPC composed of two types of SNG materials. The grey and white areas are corresponding to the allowed and forbidden bands, respectively. The band edges move to higher frequency when $\Omega > 1.96$, while move to lower frequency when $\Omega < 0.812$. Since materials A and B are PIMs (NIMs) when $\Omega > 1.96$ ($\Omega < 0.812$), according to discussions in Section 3, there are no complete gaps in these two frequency ranges. On the other hand, there exist two complete gaps marked as II and III at the range of (0.812, 1.96). The up edge of gap II moves to upper frequency, the low edge of gap II moves to lower frequency. And the up edge of gap III moves to upper frequency, the low edge of gap III moves to lower frequency. The allowed band between gaps II and III is getting narrower and narrower; the gaps II and III are getting wider and wider. The complete gaps, thus, appear for TE and TM polarizations simultaneously.

In order to understand the physics mechanism of the complete gaps, we investigate the distributions of electric fields inside the finite 1DPCs at some frequencies of the band edges at normal incidence. We plot the electric fields of the band edges of these complete gaps in Fig. 5. The electric fields inside the 1DPC of $(AB)^{16}$ at different frequencies (a) $\Omega = 2.46995$ is the up band edge of gap I in Fig. 4; (b) $\Omega = 1.84688$ is the low band edge of the gap II in Fig. 4; (c) $\Omega = 1.28366$ is the up band edge of the gap III in Fig. 4. We can see that the electric fields of two complete gap edges [Figs. 5(b) and (c)] are quite similar but are very

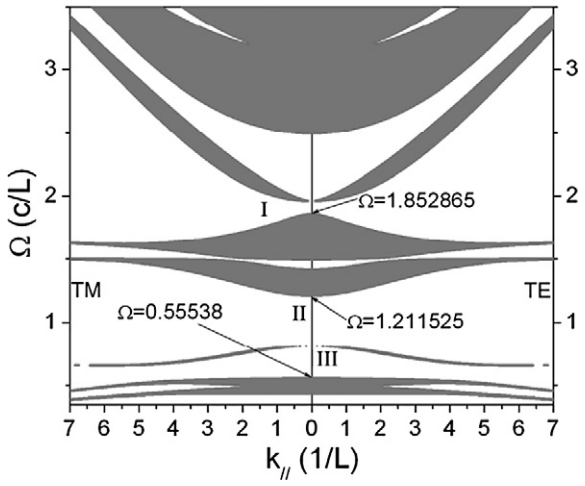

Fig. 6. Projected band structure of one-dimensional photonic crystal composed of three different types of materials (ABC), C is PIMs, A and B are SNG materials with the parameters: $d_A = d_B = 0.45L$, $d_C = 0.1L$, $\varepsilon_C = 1.0$, $\mu_C = 1.0$.

different from that of Bragg gap [Fig. 5(a)]. The electric fields of Bragg gap edge reach maxima inside material B. The electric fields of complete gap edges are rapidly changing at the interferences, and reach maxima at the interfaces of ENG and MNG materials. As is well known, the electromagnetic waves are evanescent in SNG materials. Unlike the Bragg gap, these complete gaps originate from interactions of forward-decaying and backward-decaying evanescent waves, which lead that the electric fields localize at the interfaces of ENG and MNG materials.

5. Complete gaps in three-constituent 1DPC

In the above, we have considered 1DPC composed of ENG and MNG materials. Now, we further consider a three-constituent periodic structure which is composed of three kinds of materials $(ABC)^N$. Dielectrics A and B are still SNG materials as given in the foregoing discussion, and C is PIMs. Then using transfer matrix method, we can get the dispersive relation

$$\begin{aligned} 2\cos(KL) = {} & 2\cos(k_A d_A)\cos(k_B d_B)\cos(k_C d_C) \\ & - \left(\frac{\sigma_B}{\sigma_A} + \frac{\sigma_A}{\sigma_B}\right)\sin(k_A d_A)\sin(k_B d_B)\cos(k_C d_C) \\ & - \left(\frac{\sigma_C}{\sigma_B} + \frac{\sigma_B}{\sigma_C}\right)\cos(k_A d_A)\sin(k_B d_B)\sin(k_C d_C) \\ & - \left(\frac{\sigma_C}{\sigma_A} + \frac{\sigma_A}{\sigma_C}\right)\sin(k_A d_A)\cos(k_B d_B)\sin(k_C d_C), \end{aligned} \tag{4}$$

the symbols in this equation have the same meaning as that in Eq. (2). Fig. 6 shows the band structure of the three-constituent 1DPC. One can see that there are three complete gaps, denoted as gaps I, II and III, respectively. Gaps I and II are still in the frequency range (0.812, 1.96), while gap III is in the range below 0.812.

We continue to study the physics mechanism of these complete gaps. We plot Fig. 7 to show the behaviors of electric fields inside the finite 1DPCs of $(ABC)^{16}$ at some frequencies of the band edges at normal incidence. We choose the frequencies (a) $\Omega = 0.55538$ is the low band edge of the gap III in Fig. 6; (b) $\Omega = 1.211525$ is the up band edge of the gap II in Fig. 6; (c) $\Omega = 1.852865$ is the low band edge of the gap I in Fig. 6. The electric fields (a), (b) and (c) in Fig. 7 are quite similar with the electric fields (a), (b) and (c) in Fig. 5, respectively. Complete gaps I and II are still evanescent-wave-assisted complete gaps, they result from evanescent wave tunneling. Gap III is a complete Bragg gap.

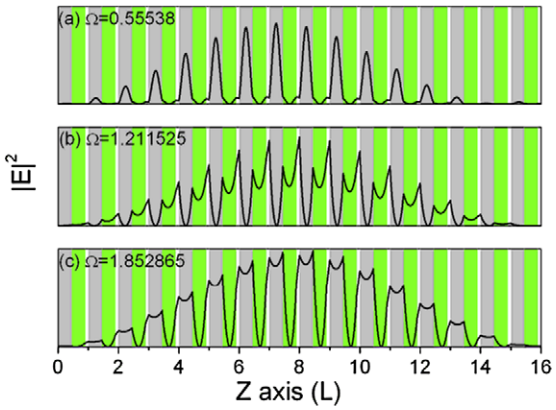

Fig. 7. Electric fields inside the 1DPC of $(ABC)^{16}$ at different frequencies: (a) $\Omega = 0.55536$ is the low band edge of the gap III in Fig. 6. (b) $\Omega = 1.211525$ is the up band edge of the gap II in Fig. 6. (c) $\Omega = 1.852865$ is the low band edge of the gap I in Fig. 6.

Now, we analyze the formation of complete Bragg gap in this three-constituent 1DPC. When adding the third material C, the 1DPC is alternating stacked by two types of SNG media and PIMs. In the frequency range $(0.35, 0.812)$, the unit cell of this 1DPC is composed of NIM–NIM–PIM, and two NIMs have the same refraction index. Therefore, this 1DPC can be dealt with the one composed of NIM–PIM. In NIM, the electromagnetic waves are backward, since the energy flux and wave vector have the opposite directions [8], whereas these vector have the same directions in PIM. The formation of this complete gap can be understood by the absence of fundamental mode in a waveguide whose core is made of NIM materials, which have been pointed out in Refs. [13,14]. Therefore, using this three-constituent model, two types of complete gaps can be obtained easily. Not only the Bragg complete gap appear, which have been found in the previous report [13], but also the complete evanescent tunneling gap occur, which is a new type complete gap.

6. Discussion and conclusion

In conclusion, we have shown that a new type of complete gap is found in one-dimensional photonic crystals composed of two kinds of SNG materials. The complete gaps originate from the evanescent wave tunneling in the single-negative materials. The complete gaps are obtained simultaneously for TE and TM polarizations. A three-constituent 1DPC composed of two types of SNG materials and PIMs is also studied. Two kinds of different complete gaps can be found in this three-constituent 1DPC. The study of complete gaps will be useful for a deeper understanding of the properties of single negative materials.

Quite recently, it is shown that negative index metamaterials can be realized in the visible [17,18]. We will discuss the possible application of our model. Take Fig. 4(b) in Ref. [18] for example. In the 'secondary' linear polarization, which is orthogonal to the primary polarization of the incident light [18], the sample's behavior is single negative. Namely the effective permeability (μ') is positive, and the permittivity (ε') is negative. If the other type of SNG can be fabricated, whose permeability and permittivity satisfy the relation $\mu = \varepsilon'$, $\varepsilon = \mu'$, then, the 1DPCs made by these two materials can exhibits complete gaps in the visible. And the 1DPCs with two types of complete gaps can also be fabricated with the similar method. We believed our model can be experimentally verified in the visible with the development of advanced nanofabrication technologies and lead to possible application in the future.

Acknowledgements

This work was supported by the National Natural Science Foundation of China (10674183), the National 973 Project of China (2004CB719804), the Ph.D. Degrees Foundation of Ministry of Education of China (20060558068).

References

[1] Yablonovitch, Phys. Rev. Lett. 58 (1987) 2059.
[2] S. John, Phys. Rev. Lett. 58 (1987) 2486.
[3] J.D. Joannopoulos, P.R. Villeneuve, S. Fan, Nature (London) 386 (1997) 143.
[4] Y. Fink, J.N. Winn, S. Fan, C. Chen, J. Michel, J.D. Joannopoulos, E.L. Thomas, Science 282 (1998) 1679.
[5] H.T. Jiang, H. Chen, H.Q. Li, Y.W. Zhang, S.Y. Zhu, Appl. Phys. Lett. 83 (2003) 5386.
[6] L.G. Wang, H. Chen, S.Y. Zhu, Phys. Rev. B 70 (2004) 245102.
[7] L. Wu, S. He, L. Shen, Phys. Rev. B 67 (2003) 235103.
[8] V.G. Veselago, Sov. Phys. Usp. 10 (1968) 509.
[9] D.R. Smith, N. Kroll, Phys. Rev. Lett. 85 (2000) 2933.
[10] J.B. Pendry, Phys. Rev. Lett. 85 (2000) 3966.
[11] R.A. Shelby, D.R. Smith, S. Schultz, Science 292 (2001) 77.
[12] J. Li, L. Zhou, C.T. Chan, P. Sheng, Phys. Rev. Lett. 90 (2003) 083901.
[13] I.V. Shadrivov, A.A. Sukhorudov, Y.S. Kivshar, Phys. Rev. Lett. 95 (2005) 193903.
[14] I.V. Shadrivov, A.A. Sukhorudov, Y.S. Kivshar, Phys. Rev. E 67 (2003) 057602.
[15] V.M. Shalaev, W. Cai, U.K. Chettiar, H.K. Yuan, A.K. Sarychev, V.P. Drachev, A.V. Kildishev, Opt. Lett. 30 (2005) 3356.
[16] G. Dolling, C. Enkrich, M. Wegener, C.M. Soukoulis, S. Linden, Opt. Lett. 31 (2006) 1800.
[17] G. Dolling, C. Enkrich, M. Wegener, C.M. Soukoulis, S. Linden, Opt. Lett. 32 (2007) 53.
[18] U.K. Chettiar, A.V. Kildishev, H.K. Yuan, W. Cai, S. Xiao, V.P. Drachev, V.M. Shalarv, Opt. Lett. 32 (2007) 1671.
[19] N.H. Liu, Phys. Rev. B 55 (1997) 4097.
[20] J.W. Dong, H.Z. Wang, Appl. Phys. Lett. 91 (2007) 111909.
[21] A. Alú, N. Engheta, IEEE Trans. Antennas Propagat. 51 (2003) 2558.
[22] A. Grbic, G.V. Eleftheriades, Phys. Rev. Lett. 92 (2004) 117403.